6th International Conference on Fundamentals and Development of Fuel Cells, FDFC2015
3 to 5 February, 2015, Toulouse, FRANCE

Numerical modelling of membrane degradation in PEM water electrolyzer: Influence of the temperature and current density

M. Chandesris, V. Médeau, N. Guillet, S. Chelghoum, D. Thoby, F. Fouda-Onana
Univ. Grenoble Alpes F-38000 Grenoble, France
CEA, LITEN, DEHT, F-38054 Grenoble, France
marion.chandesris@cea.fr

Keywords: PEM Electrolyser, Modelling, Membrane degradation, Experimental validation.

ABSTRACT

A 1D polymer electrolyte membrane water electrolyzer (PEMWE) model that incorporates chemical degradation of the membrane is developed to study the influence of temperature and current density on the membrane degradation. The development of the model is supported by specific single cell experiments to both validate the different modeling assumptions and determine some of the physical parameters involved in the performance and degradation models. The model is then used to study the time evolution of the membrane thickness. The coupling between the performance and the chemical degradation models allows capturing the acceleration of membrane thinning.

1. INTRODUCTION

PEM water electrolyzers (PEMWEs) are considered as a viable alternative for generation of hydrogen from renewable energy sources. Indeed they present many advantages over other available technologies (simplicity, excellent dynamic response to power fluctuations, possibility of compact design, ...) making them ideal for operation with intermittent renewable energy sources such as wind and solar power.

Recent impressive progresses have demonstrate the potentiality of PEMWE technology [8] and on-going efforts are devoted to search novel solutions to reduce the costs of the systems while maintaining high durability life-time. While performance can be tested quite rapidly, lifetime estimation is much more difficult to evaluate, with a typical degradation characteristic time of thousands of hours for PEMWEs, compared to hundreds of hours in PEMFC. Thus, lifetime estimation of the different components requires long and costly experiments, whereas it remains crucial to determine the service life of the electrolyzer. In this context, modeling of degradation mechanisms in PEMWE is a very useful tool to predict the performance of the system over its lifetime depending on the operating conditions.

Several performance PEMWE models have been reported in the literature [3] [2] [5] [1] [4]. These models are based on thermodynamic principles and Butler-Volmer kinetics and allow for simulating the electrochemical behavior of the electrolyzer depending on the operating conditions (mainly temperature and pressure). Regarding degradation mechanisms as for PEM fuel cell, there is not a unique cause of degradation: catalysts and catalyst layers degradation, membrane degradation, current collectors corrosion. Nevertheless, in PEMWEs, performance decreases and durability restrictions are mostly attributed to membrane pollution or degradation, reason why we will focus on this mechanism. The main idea is to propose a mechanistic model of membrane chemical degradation and to develop this model in a 1D MEA performance model in order to obtain an explicit coupling between membrane degradation and the performance of the electrolyzer. The aim is to provide some insight on the parameters affecting the membrane degradation. The development of the model is

supported by specific single cell experiments to both validate the different modeling assumptions and determine the different physical parameters involved in both the performance and the degradation models.

2. SINGLE CELL EXPERIMENTAL SET-UP

Chemical membrane degradation at various temperatures and current densities is investigated using a 25 cm² single cell set-up. During experiments, only the anode is supplied with deionized water at a constant flow rate of 200 $ml.h^{-1}$. Water will be collected at both the anode and cathode sides since water crosses the membrane during electrolysis operation. Two MEAs, provided by Johnson Mattey, have been studied. Anode and cathode catalysts loading are almost the same for the two samples: 1.94 mg/cm² of IrO_2 black and 1.19 mg/cm² of Pt black for sample JM 3.4 and 1.99 mg/cm² of IrO_2 black and 1.31 mg/cm² of Pt black for sample JM 3.2. Both MEAs are made of a Nafion N117 membrane. Electrolysis performance of the MEAs is evaluated at beginning of life (BoL) by measuring polarization curves at three different temperatures: 313, 333 and 353K. The two MEAs have the same performance at BoL. Electrochemical impedance spectroscopy (EIS) are also carried at BoL at different temperatures using a high current potentiostat (Bio-Logic Science Instruments SAS, HCP-803, 80 A) at frequencies ranging from 10 kHz to 200 mHz.

The chemical degradation is characterized by regularly collecting the effluent water of the cell at the anode and at the cathode sides and by measuring the fluoride release rate in the samples using a fluoride selective electrode. A constant current density is applied during approximately 200 to 300 hours, until a sufficient number of water samples is gathered and then the current density is changed. The two MEAs have been aged at 353 K and 333K respectively. The fluoride-ion release rate (FRR) is calculated from the flow rate of the collected water and the concentration of F^- ions. The obtained results are presented in Fig. 1. The FRRs from the cathode is obviously far larger than the one at the anode and the temperature has also a strong impact on the membrane degradation, as has been already reported for electrolyzer by [7]. Increasing the temperature clearly accelerates the membrane degradation. A clear influence of the current density on the FRR can also be observed. The effect of the current density on membrane degradation is summed up Fig. 2 where the sum of the averaged measured FRRs at the anode and at the cathode is presented versus the current density. At both temperatures, the FRR increases as the current density decreases. At 353K, it reaches a maximum around 0.4 A/cm² and then decreases. At 333K, the maximum is reached at a lower value, around 0.2 A/cm².

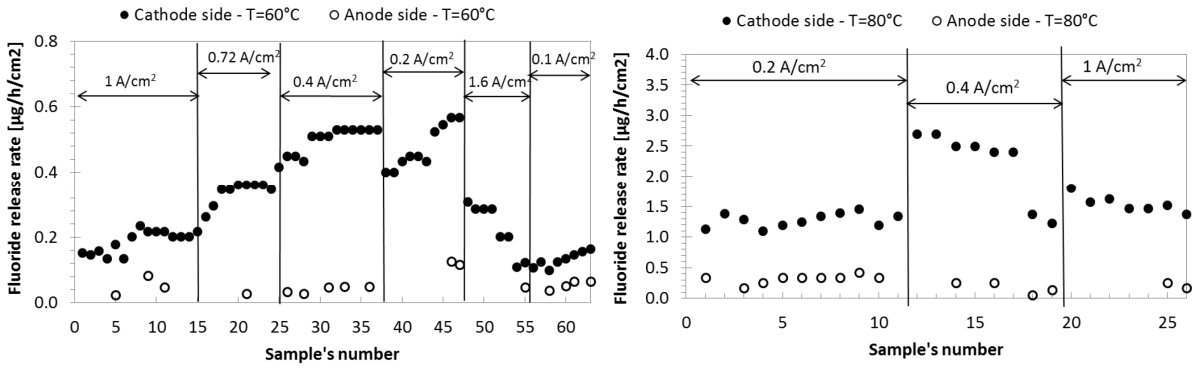

Figure 1. Fluoride-ion release rates in the effluent water at the anode and the cathode.

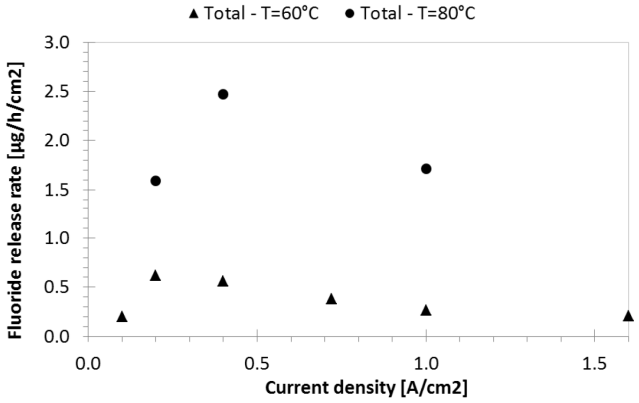

Figure 2. Fluoride-ion release rates in the effluent water at the anode and the cathode.

3. PEM WATER ELECTROLYZER PERFORMANCE MODEL

The purpose of the performance model is to correctly account for the electrochemical behavior of the electrolyzer to later be able to study the coupling between the membrane degradation and the PEMWE performance. To simplify the performance model, we assume that the activity of the different products and reactants can be set equal to one in PEM water electrolysis. With this assumption, the modeling of gas and liquid transport in the cell is not needed to account for cell polarization curves. Electronic and ionic transports through the different cell components are considered together with the electrochemical behavior of the anodic and cathodic catalyst layers which are modelled using the Butler-Volmer expression:

$$i = i_{oj}\gamma_j\left[\exp\left(\frac{\alpha_j zF}{RT}\eta_j\right) - \exp\left(-\frac{(1-\alpha_j)zF}{RT}\eta_j\right)\right] \quad (1)$$

where the subscript j is equal to A at the anode and C at the cathode. The overpotential η_j is deduced from the local ionic and electric potentials and from the reversible potential given by Nernst equation.

The results of the performance model directly depend on the physical properties of the different components of the tested MEA: thickness and ionic conductivity of the membrane, thickness and electronic conductivity of the two current collectors, electrochemical properties of the catalyst layers. These physical properties are determined based on the results of the single cell experiments and literature data. As can be seen Fig. 3, the present performance model is able to capture the polarization curves obtained experimentally for the three different temperatures. In particular, the behavior at low current density, characteristic of the electrochemical model, is well captured as can be seen using a logarithmic scale.

4. MEMBRANE DEGRADATION MODEL

One of the most complete studies that gives evidence of membrane degradation in PEMWE was conducted at PSI in the 1990's [11] where substantial thinning of the membranes has been detected. Regarding the dissolution process, the ion exchange capacity measurements on thinned membranes reveal that the composition of the remaining polymer is not changed with respect to ionic groups. Furthermore, complementary experiments indicated that the membrane degrading reaction can be localized on the cathode side of the cell, as is also obtained in the experimental part of the present study. The following scenario will thus be considered in the model: oxygen cross-over from the anode to the cathode side, production of

hydrogen peroxide H_2O_2 at the cathode side, formation of free radicals that attack the membrane on the surface without altering the transport properties of the membrane, leading to fluoride release and thinning of the membrane.

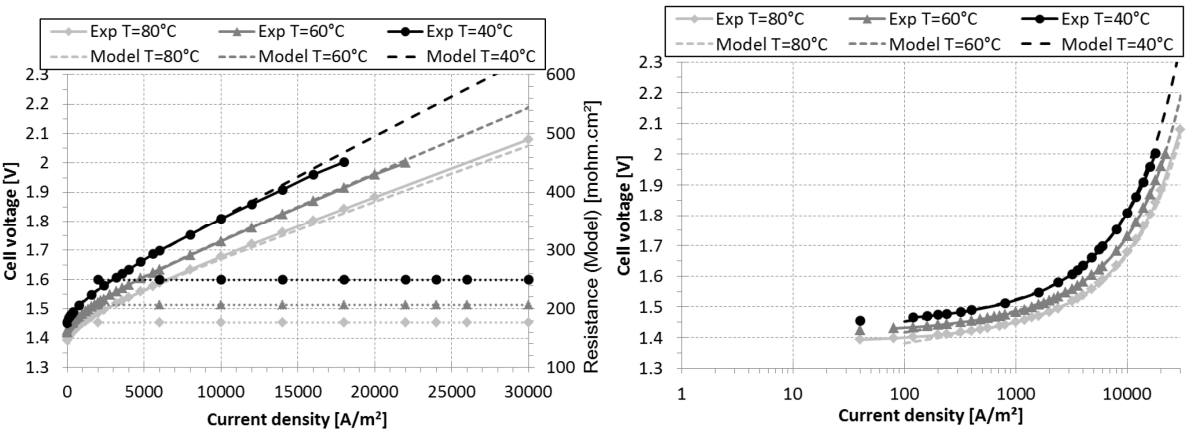

Figure 3. Experimental and simulated cell potentials at different temperatures. The behavior at low current density, characteristic of the electrochemical model, is displayed at the right using a log scale.

4.1 Gas cross-over

One of the roles of the membrane is the separation of gases between the anode and the cathode sides. However, Nafion cannot prevent the oxygen and hydrogen to permeate between the electrodes. The transport of dissolved gases in the membrane is modeled taking into account diffusion as well as water transport. The concentration of solved species in each side of the membrane is obtained using Henry's law and the partial pressure. A mass balance of fluxes is written for both O_2 and H_2 on each side of the membrane to determine the partial pressure of each gas in each compartment (anode and cathode). The obtained molar fractions for O_2 on the cathode side, respectively H_2 on the anode side, in function of the current density are presented in Fig. 4. The expected decrease with the current density is recovered. At very low current density, a very high molar percentage is observed due to the fact that a smaller amount of the other gas is produced. A strong difference between O_2 and H_2 molar fractions can be observed. This is due to the fact that the permeation coefficient and the source term are greater for H_2. The model is also as expected strongly temperature dependent.

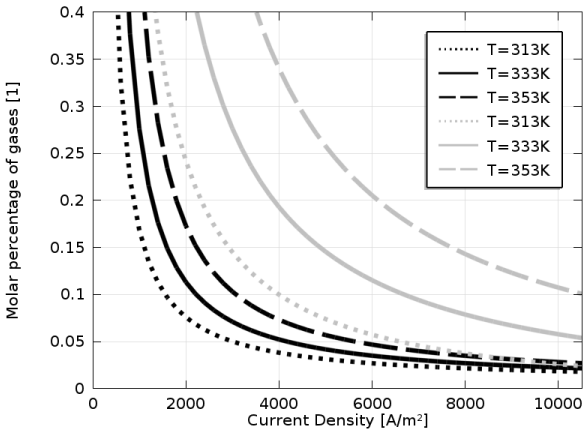

Figure 4. Comparison between O_2 (black) and H_2 (grey) molar percentage respectively at the cathode and anode sides.

4.2 Hydrogen peroxide formation

Once arrived at the cathode side, oxygen is involved into oxygen reduction reactions (ORR) which can occur through a 2 or a 4-electron exchange reaction. The cathode side is at very low potential (< 0V vs. SHE), as hydrogen evolution reaction occurs at the platinum electro-active sites. At potential lower than 0.4 V, ORR is considered to predominantly occurs via H_2O_2 formation pathway and one can neglect water recombination. The electrochemical formation rate of H_2O_2 is modeled as in [10] using a simple order kinetic law and assuming that the reverse reaction is negligible.

4.3 Radical formation and membrane attack

The decomposition of hydrogen peroxide into hydroxyl and hydroperoxyl ($HO^{\cdot}$ and $HOO^{\cdot}$) radicals has already been widely studied. In the present study, we consider decomposition of hydrogen peroxide with and without the presence of metal ions (in our case Fe^{2+}). The direct reaction is kinetically very low compared to those in presence of ferrous ions. Those ferrous ions could arise from the manufacturing process, the metallic pipes supplying the water or the corrosion of the end plates. The chemical reactions involving the radicals and their associated kinetic constants are taken from the work of Gubler *et al.* [6] and are presented in Table 1. All the kinetic constants are given at 298 K as reported in [6], except for the kinetic constant of reaction 3, which is an important reaction and for which its temperature dependency has been found in the literature [9]. The reaction rates of the different chemical reactions ν_i are all assumed to follow a simple order kinetic law regarding the reagents concentrations. The time evolution of the concentration of the different species present in the cathode catalyst layer (H_2O_2, $HO^{\cdot}$, $HOO^{\cdot}$, Fe^{2+} and Fe^{3+}) is obtained by writing the molar mass balance equation of each specie over the thickness of the cathode catalyst layer, which is modeled here as an interface.

Table 1. Overview of the reactions involving free radicals and their associated kinetic constants

#	Reaction	Rate constant
2	$H_2O_2 \rightarrow 2HO^{\bullet}$	$k_2 = 1.2 \times 10^{-7} (s^{-1})$
3	$H_2O_2 + Fe^{2+} \rightarrow Fe^{3+} + HO^{\bullet} + HO^{-}$	$k_3 = 1.05 \times 10^{8} \exp(-9460/RT)$ $(l.mol^{-1}\ s^{-1})$
4	$H_2O_2 + Fe^{3+} \rightarrow Fe^{2+} + HOO^{\bullet} + H^{+}$	$k_4 = 4 \times 10^{-5} (l\ mol^{-1}\ s^{-1})$
5	$HO^{\bullet} + Fe^{2+} \rightarrow HO^{-} + Fe^{3+}$	$k_5 = 2.3 \times 10^{8}$ $(l\ mol^{-1}\ s^{-1})$
6	$HO^{\bullet} + H_2O_2 \rightarrow HOO^{\bullet} + H_2O$	$k_6 = 2.7 \times 10^{7} (l\ mol^{-1}\ s^{-1})$
7	$HO^{\bullet} + O_2 \rightarrow HOO^{\bullet} + H_2O$	$k_7 = 1.2 \times 10^{10} (l\ mol^{-1}\ s^{-1})$
8	$HOO^{\bullet} + Fe^{3+} \rightarrow Fe^{2+} + O_2 + H^{+}$	$k_8 = 2 \times 10^{4} (l\ mol^{-1}\ s^{-1})$
9	$HOO^{\bullet} + Fe^{2+} + H^{+} \rightarrow Fe^{3+} + H_2O_2$	$k_9 = 1.2 \times 10^{6} (l\ mol^{-1}\ s^{-1})$
10	$HO^{\bullet} + R_f - CF_2 - COOH \rightarrow products$	$k_{10} \leq 10^{6} (l\ mol^{-1}\ s^{-1})$

The source of metallic ion is an important parameter of the model, as the final degradation rate appears to be almost proportional to it. In absence of experimental data, the source term has been fitted in order to correspond to expected values of Fe^{2+} concentration and overall degradation. Furthermore, different source terms will be considered: a constant source term, an imposed inlet concentration and a condition dependent source term.

The impact, in term of membrane degradation and fluoride release of reaction #10 is evaluated assuming that reaction #10 cuts the side chain. We evaluate that the global mechanism uses 12.5 $HO^{\cdot}$ for the entire unzipping of the side chain plus corresponding backbone. As a consequence, the Fluor release rate will be taken equal to 3.6 times the kinetic rate of the 10th reaction.

4.4 Results and discussion

Fig. 5 presents a comparison between the experimental and the simulated fluoride release rates obtained at 353K. These simulations results are obtained using a constant source term of Fe^{2+} fitted to 9.10^{-2} mol/m^3/s and 20% variations around this value are also displayed for comparison. The model is able to capture the current density effect on the Fluoride release rate. At very low current density, the degradation rate is low, and then it increases as the current density increases to reach a maximum at quite low current density and then decreases. At high current density, we were expecting a decrease in the Fluoride release since the molar percentage of oxygen at the cathode decreases and thus the peroxide formation. However, at low current density, the observed behavior was not expected. To understand the overall shape of the curve, the reaction rates of reactions 3, 6 and 10 are also displayed Fig. 5. Reaction 3 is the main source of hydroxyl radicals $HO^{\cdot}$ along with reaction 2 whose order of magnitude is negligible in those conditions whereas reactions 6 and 10 are the two main consumption reactions for $HO^{\cdot}$ (along with reactions 5 and 7). Thus, when neglecting minor reactions, we have $v_3 = v_6 + v_{10}$, where v_{10} is the membrane degradation reaction rate. At very low current densities, reaction 6 counts for an important part of the radicals consumption. Indeed, as the concentration of H_2O_2 becomes important at very low currents, the sixth reaction rate becomes dominant compared with the reaction rate of the membrane degradation and thus consumes almost all the $HO^{\cdot}$, explaining the lower fluoride release encountered at low current densities.

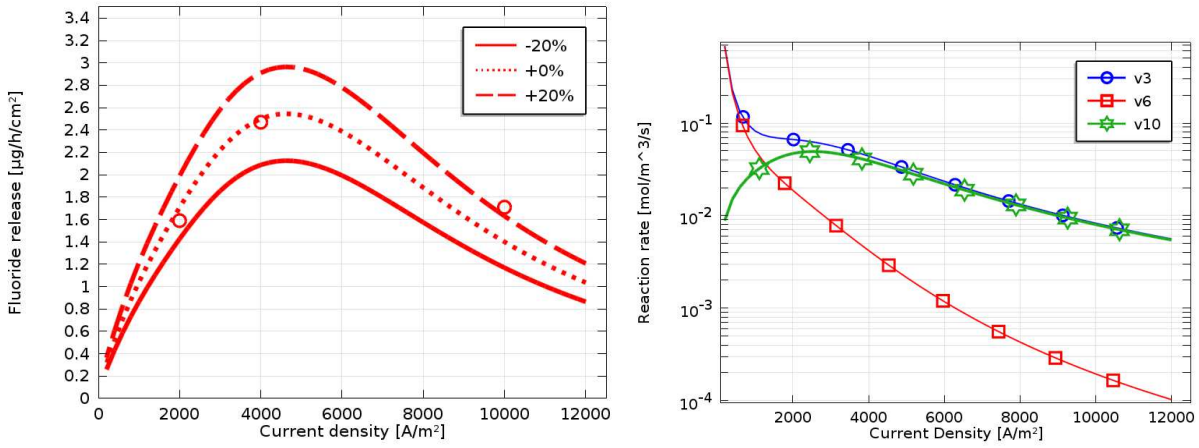

Figure 5. Left: Fluoride release at 353K with comparison to experimental points. Right: Reaction rates of reactions 3, 6 and 10

As previously pointed out, the source term of metallic ions is a significant parameter of the model and the fluoride release and degradation rates are almost directly proportional to this source term. A temperature dependent source term of Fe^{2+} can help adjust the level of degradation between several temperatures, while a current dependent one can adjust the degradation form regarding current density. In order to give an illustration, Fluoride release results obtained with three different Fe^{2+} source terms are presented in Fig. 6. The choice of one source term compared to another does not modify the overall behavior of the fluoride release rate with current density but can significantly change the position of the peak and the magnitude at one temperature compared with another.

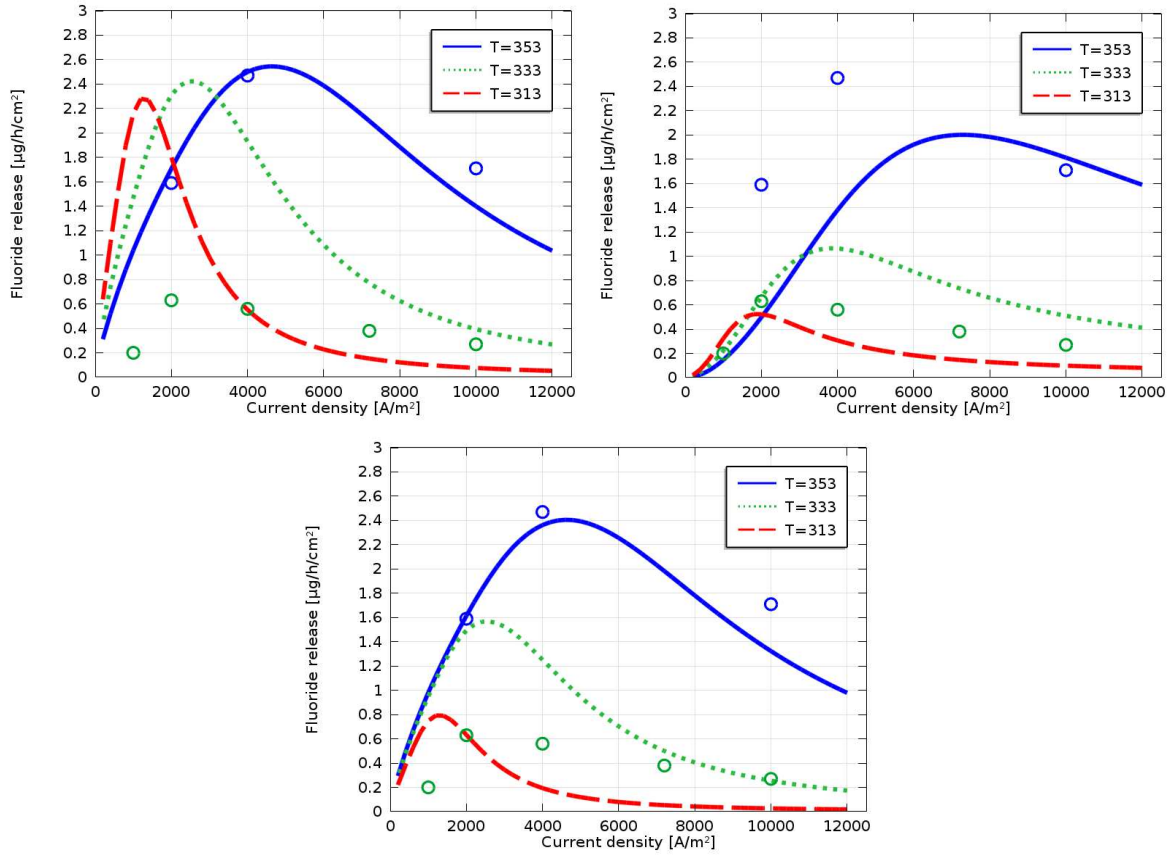

Figure 6. Experimental and simulated Fluoride release at different temperatures. Top left: Constant Fe^{2+} source term; Top right: Imposed Fe^{2+} inlet concentration (3ppm); Bottom: Temperature dependent source term of Fe^{2+}

5. MEMBRANE THINING

A 1D PEMWE model that incorporates chemical degradation of the membrane has been developed and validated against experimental data. From this physical model, the objective is now to deduce the time evolution of the membrane thickness. Indeed, as the membrane thins down, oxygen crossover increases, which accelerates the membrane degradation and thus accelerates the thinning of the membrane. The time evolution of the membrane thickness is thus expected not to be linear but exponential. Modeling the thinning of the membrane implies changes in geometry, which has been taken into account through a change of variable. By doing this, some physical constants within the membrane become time-dependent (the ionic conductivity, the diffusion coefficients and the water velocity), but the rest of the model is not modified. The time evolution of the thickness of the membrane is modeled in the following way: $\frac{de_M}{dt} = \Delta e_M R_{fluor}$, where Δe_M corresponds to the thinning of the membrane per mol of released fluor and R_{fluor} is the Fluor release in mol/s, obtained from the degradation membrane model.

Fig. 7 gives the time evolution of the membrane thickness in percentage of its initial value when operating at 1 A/cm² at 333K and 353K. As expected, the life time is significantly decreased at high temperature. The time needed to thin 50% of the membrane is around 38'500h at 333K but only 8'700h at 353K. The evolution shows the coupling effect which leads to a non-linear decrease of the membrane thickness.

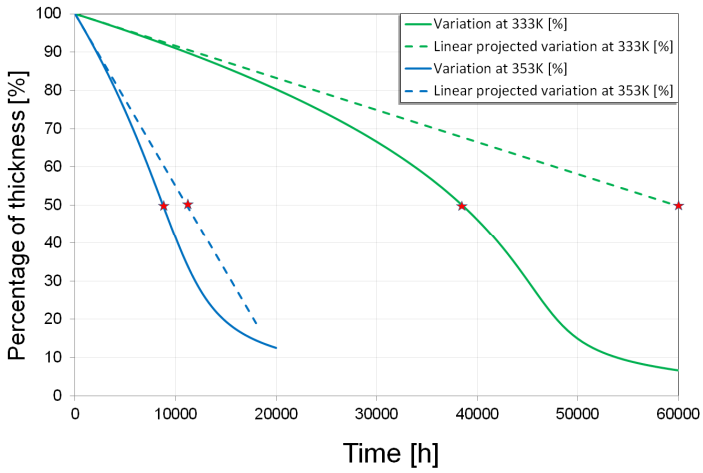

Figure 7. Time evolution of the membrane thickness in percentage at 1 A/cm² at 333K and 353K. Plain lines: coupled model taking into account the thinning of the membrane; dotted lines: linear model without the coupling with the membrane thinning

ACKNOWLEDGEMENTS

This work has been performed within the European project NOVEL. The financial support of the European 7th Framework Program (Grant Agreement 303484) and of CEA is gratefully acknowledged.

REFERENCES

[1] A. Awasthi, K. Scott, and S. Basu. Dynamic modeling and simulation of a proton exchange membrane electrolyzer for hydrogen production. *Int. J. Hydrogen Energy*, 36(22):14779–14786, 2011.
[2] C.Y. Biaku, N. V. Dale, M. D. Mann, H. Salehfar, A.J. Peters, and T. Han. A semiempirical study of the temperature dependence of the anode charge transfer coefficient of a 6 kw pem electrolyzer. *Int. J. Hydrogen Energy*, 33:4247–4254, 2008.
[3] P. Choi, D. G. Bessarabov, and R. Datta. A simple model for solid polymer electrolyte (SPE) water electrolysis. *Solid State Ionics*, 175:535–539, 2004.
[4] R. Garcia-Valverde, N. Espinosa, and A. Urbina. Simple PEM water electrolyser model and experimental validation. *Int. J. Hydrogen Energy*, 37(2):1927–1938, 2011.
[5] S.A. Grigoriev, P. Millet, S.A. Volobuev, and V.N. Fateev. Optimization of porous current collectors for PEM water electrolysers. *International Journal of Hydrogen Energy*, 34(11):4968 – 4973, 2009. 2nd International Workshop on Hydrogen, 2nd International Workshop on Hydrogen.
[6] L. Gubler, S. Dockheer, and H. Koppenal. Radical (ho, h and hoo) formation and ionomer degradation in polymer electrolyte fuel cells. *J. Electrochem. Soc*, 158(7):B755–B769, 2011.
[7] A. B. LaConti, H. Liu, C. Mittelsteadt, and R. McDonald. Polymer electrolyte membrane degradation mechanisms in fuel cells. findings over the past 30 years and comparison with electrolyzers. *ECS Trans.*, 1(8):199–219, 2006.
[8] P. Millet, R. Ngameni, S. A. Grigoriev, N. Mbemba, F. Brisset, A. Ranjbari, and C. Etievant. Pem water electrolyzers: From electrocatalysis to stack development. *Int. J. Hydrogen Energy*, 35:5043–5052, 2010.
[9] T. Rigg, W. Taylor, and Weiss J. The rate constant of the reaction between hydrogen peroxyde and ferrous ions. *The journal of chemical physics*, 22(4):575, 1954.
[10] V. Sethuraman, J. Weidner, A. Haug, A. Motupally, and L. Protsailo. Hydrogen peroxyde formation rrate in a PEMFC anode and cathode. effect of humidity and temperature. *J. Electrochem. Soc*, 155(1):B50–B57, 2008.
[11] S. Stucki, G. G. Scherer, S. Schlagowski, and E. Fischer. PEM water electrolysers: evidence for membrane failure in 100kW demonstration plants. *Journal of Applied Electrochemistry*, 28:1041–1049, 1998.